WORLD CONFERENCE ON TIMBER ENGINEERING 2025
BRISBANE, AUSTRALIA
Advancing Timber for the Future Built Environment

# Evaluation for ultimate strength for steel-plate-inserted joint with drift-pins at the end of glulam beams

W. Kambe[1]1, A. Takino[2], K. Suzuki[3], Y. Ochiai[4], S. Nakashima[5], S. Okamoto[6], K. Kobayashi[7], K. Sawata[8], K. Ogawa[9], K. Tanaka[10]

**ABSTRACT:** In this study, loading tests with steel-plate-inserted joints using drift pins at the end of glulam-beams were conducted. strength for each fracture type was calculated. Material tests were also conducted separately to obtain the 5% lower limit of splitting failure constant and shear strength. As a result, it was found that the fracture properties were determined more correctly than the current wood structure standard, to evaluate the ultimate strength more accurately.

**KEYWORDS:** Joint, ultimate strength, Splitting strength, Shear strength, Drift-pins

## 1 – INTRODUCTION

This study focuses on the ultimate strength of steel-plate-inserted joints with drift-pins at the end of a glulam beams. Since the ultimate strength those joints greatly affects the performance of a structure, it is important to evaluate it accurately. It is said that those joints would fail in splitting or shear fracture, those fracture types are ultimate conditions[1]. However, it is difficult to clearly define the fracture properties, which leads to design difficulties. This study examines the splitting and shear resistance of the joints by conducting load tests on the joints and discusses the evaluation method of the ultimate strength capacity of the joints.

### Strength equation

The Strength equations for joints specified in the current Standard for Structural Design of Timber Structures are presented in Equations (1) to (3). Equation (2) represents the splitting strength formula, while Equation (3) corresponds to the shear strength formula. As indicated in Equation (1), the smaller of these two values determines the design strength[1].

$$P_{uw}=\min\{ P_{uw1}, P_{uw2}\} \quad (1)$$

$$P_{uw1} = \frac{2}{sin\alpha} \cdot C_r \cdot l \sqrt{h_e/\left(1-{h_e}/{h}\right)} \quad (2)$$

$$P_{uw2} = \frac{2}{3sin\alpha} \cdot \xi \cdot h_e \cdot l \cdot F_s \quad (3)$$

Here, $C_r$ represents the splitting fracture constant, $h$ is the member depth, and $h_e$ is the distance from the loaded edge to the farthest fastener. Additionally, $l$ denotes the main member thickness, $F_s$ is the shear strength, and $\xi$ represents the shear force ratio (which is 1 for the tested joint specimens). The parameter $\alpha$ indicates the angle between the loading direction and the wood grain (90 degrees for the tested joint specimens). Refer to **Fig.1** For $h$, $h_e$ and $\alpha$.

[1] Wataru Kambe, College of Arch. And Env. Design, Kanto Gakuin Univ., Yokohama, Japan, wkambe@kanto-gakuin.ac.jp

[2] Atsuo Takino, Faculty of Eng., Osaka Institute of Technology, Osaka, Japan, atsuo.takino@oit.ac.jp

[3] Kento Suzuki, F.F.P.R.I., Tsukuba, Japan, suzukik777@ffpri.affrc.go.jp

[4] Yo Ochiai, Tokyo city Univ., Tokyo, Japan, ochiaiy@tcu.ac.jp

[5] Shoichi Nakashima, BRI, Tsukuba, Japan, nakas@kenken.go.jp

[6] Shigefumi Okamoto, Grad school of Human life sci., Osaka metropolitan univ., Osaka, Japan, okmt@omu.ac.jp

[7] Kenji Kobayashi, Shizuoka Univ., Shizuoka, Japan, kobayashi.kenji.b@shizuoka.ac.jp

[8] Kei Sawata, Hokkaido univ., Sapporo, Japan, ksawata@agr.hokudai.ac.jp

[9] Keita Ogawa, Shizuoka univ., Shizuoka, Japan, ogawa.keita@shizuoka.ac.jp

[10] Kei Tanaka, Oita univ., Oita, Japan, kei@oita-u.ac.jp

https://doi.org/10.52202/080513-0607

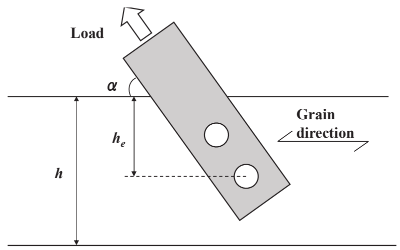


**Fig.1 Symbols Used in the Splitting Strength Formula**

When a loading test is conducted on joints, cracks typically develop in the wood at the connection. However, since the crack patterns are not necessarily uniform, it is often challenging to clearly distinguish between splitting failure and shear failure. This ambiguity has led to concerns that the complexity of structural calculations poses difficulties for designers.

To identify the conditions under which failure modes occur, joint specimens with systematically arranged drift pins were prepared and subjected to loading tests. Through detailed observations of these specimens, an attempt was made to define the characteristics of failure modes.

Material tests were also conducted to obtain failure parameters and shear strength. Several test conditions were established during the experiments. Based on the results, the input values for the strength equations of the joints were determined.

## 2 – Material tests

The material strength used in the ultimate strength equation for steel-plate-inserted joints in this study are the Fracture parameter $C_r$ and the shear strength $F_s$. The splitting failure parameter is obtained from the method given in the AIJ code [1], and the shear strength is obtained from the inverse symmetric four-point loading method given in the manual of the Japan Housing and Wood Technology Center (HOWTEC Method) [2].

### 2.1 Fracture parameter

The dimensions of the specimens used in this study are shown in the upper part of **Fig.2**, the test setup is shown in the lower part of **Fig.2** and **Fig.3**, and the specimen dimensions are shown in **Table 1**. The test parameters used here are lumber width and drift pin diameter. The material widths are 60 mm and 120 mm, and the drift pin diameters for the force are φ16, φ18, and φ20.

The material used is a species of red spruce, E95-F315 laminated wood of the same grade composition as specified in the Japanese Agricultural Standard (JAS) [3] for laminated wood. The average density was 0.55 g/cm$^3$. The number of specimens was 18 in total, with three specimens for each parameter. The edge distance of each specimen is 15 times the drift pin diameter, and the edge distance is 4 times the drift pin diameter. The failure parameters are calculated using Equation (4).

$$C_r = F_u / \left(2 \cdot l \cdot \sqrt{h_e}\right) \quad (4)$$

Here, $F_u$: Maximum load, $l$: width

Examples of fracture conditions are shown in **Fig. 4**, examples of load-deformation relationships in **Fig. 5**, relationships between fracture parameters and density in **Fig. 6**, and a list of test results in **Table 2**. The dashed line in **Fig. 6** represents the failure parameter values for this material as specified in the Standard for Structural Design of Timber Structures. These values were found to be larger than those given in the standard. Using the method specified in the Standard for Structural Design of Timber Structures (Equation (5))[1], the 5% lower bound value for the test results was calculated.

5%lower value=Ave.-$K \cdot SD$ (5)

Here, $K$: Factor indicated in AIJ code [1], SD: Standard of deviation

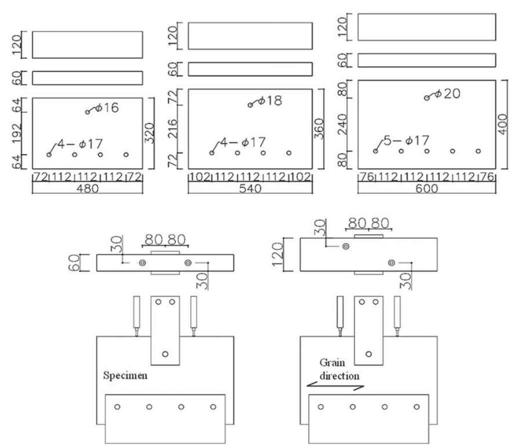


**Fig.2 Specimens for fracture parameter**

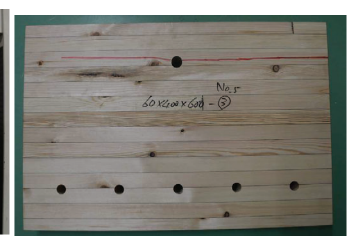

**Fig.3 Exp. setup** **Fig.4 Fracture condition**

**Table1 Specimens for fracture parameter**

| Diameter [mm] | width [mm] | length [mm] | height [mm] | edge distance [mm] |
|---|---|---|---|---|
| 16 | 60 or120 | 480 | 320 | 64 |
| 18 | 60 or120 | 540 | 360 | 72 |
| 20 | 60 or120 | 600 | 400 | 80 |


https://doi.org/10.52202/080513-0607

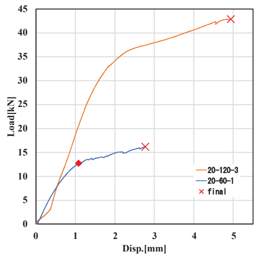


Fig.5 load-disp. Curve

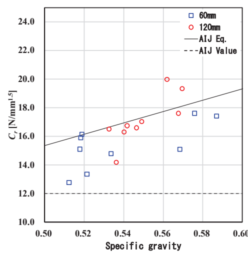


Fig.6 Test results

**Table 2 Test results**

| Width [mm] | Diameter [mm] | $C_r$ [N/mm$^{1.5}$] Ave. | S.D. | 5% lower |
|---|---|---|---|---|
| 60 | 16 | 16.3 | 1.9 | 12.6 |
| | 18 | | | |
| | 20 | | | |
| 120 | 16 | | | |
| | 18 | | | |
| | 20 | | | |

## 3.2 Shear strength

For the shear test, **Fig.7** shows an overview of the test method, **Fig.8** shows the test conditions, and **Table 3** shows the dimensions and shear span ratios of the specimens. The glued laminated timbers used were of the same grade composition as in JAS [3], E95-F315, and of the same species of Pinus sylvestris. The specimens were 120 mm in width and 200, 300, and 600 mm, with three specimens of each specification. Shear stress and apparent shear strain were determined from Eq. 6) and 7) [2] respectively. The width of the fulcrum is 200 mm.

$$F_s = \frac{3F_{ult}}{4A} \qquad (6)$$

$$Shear\ strain = \frac{\Delta\delta}{\Delta x} \qquad (7)$$

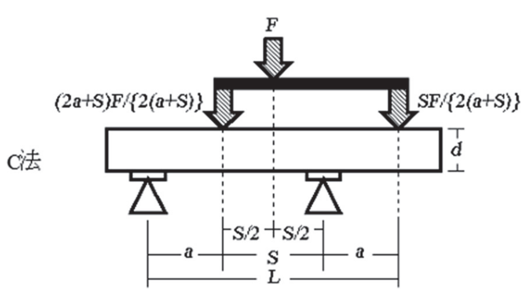


Fig. 7 Overview of the shear test method [2]

Fig.8 Shear test setup

**Table 3 Tests parameter**

| Width [mm] | height [mm] | length [mm] | a [mm] | Shear span ratio |
|---|---|---|---|---|
| 120 | 200 | 2400 | 600 | 3 |
| | 300 | 3300 | 900 | 3 |
| | 600 | 6000 | 1333 | 2.22 |


Fig.9 Fracture conditions

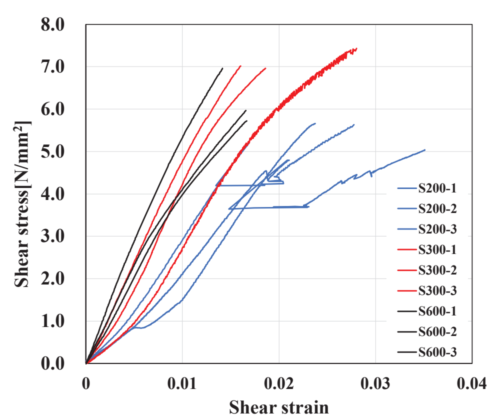


Fig.10 Stress-shear strain curves

**Table4 Test results of shear tests**

| height [mm] | Shear strength [N/mm$^2$] | | |
|---|---|---|---|
| | Ave. | S.D. | 5% lower |
| 200 | 5.44 | 0.35 | 4.34 |
| 300 | 7.14 | 0.26 | 6.32 |
| 600 | 6.22 | 0.65 | 4.16 |

## 4 – loading tests using steel-plate-inserted joint with drift-pins at the end of glulam beams

In this study, specimens were prepared using a steel-inserted joint with drift pins at the beam ends of glued laminated timber (GLT) and subjected to monotonic vertical loading tests. The test setup is shown in **Fig.11**.

Regarding the beam material used in the specimens, the wood species is Pinus sylvestris, and the GLT has an asymmetric, unequal-grade composition with a JAS[3] classification of E105-F300. All test specimens have a beam width of 120 mm.

The drift pins have a diameter of φ16 mm and a length of 120 mm. The inserted steel plate is made of SS400 steel with a thickness of 9 mm, while the slit in the beam is 11 mm wide. The effective length in Equations (2) and (3) is 105 mm.

For the drift pin holes, the beam material was drilled with holes of the same diameter as the pins, whereas the steel plate holes were designed with a 1.5 mm clearance relative to the drift pin diameter. The drift pins were installed at the factory prior to testing.

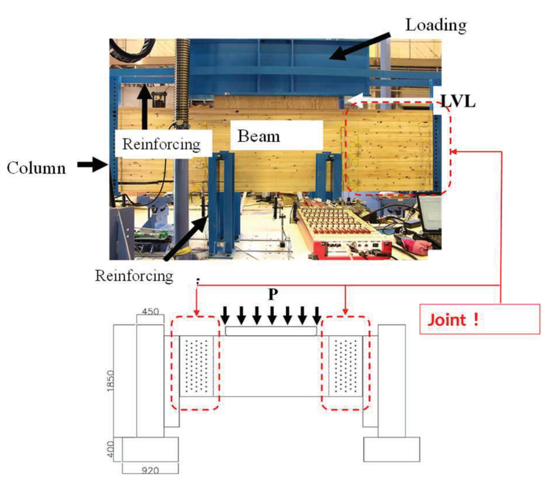


**Fig.11 Setup of loading test with joints**

### 4.1 Test parameter

In this study, joint tests were conducted in three phases. The drift pin arrangement for Phase 1 is shown in **Fig. 12**, for Phase 2 in **Fig. 13,14**, and for Phase 3 in **Fig. 15,16**.

In Phase 1, joints were installed and tested on beams with depths of 450 mm, 600 mm, 1000 mm, and 1500 mm. In Phases 2 and 3, joints were installed and tested on beams with depths of 450 mm and 600 mm. During Phase 1, lateral buckling occurred in the specimens with beam depths of 1000 mm and 1500 mm, preventing joint failure. Consequently, the analysis focused on specimens with 450 mm and 600 mm beam depths.

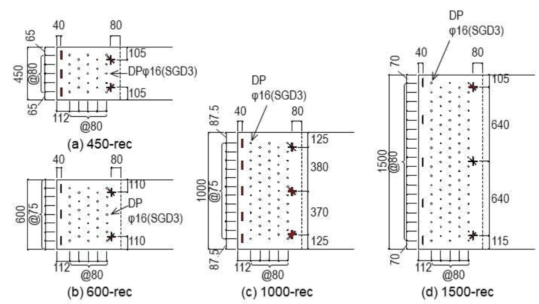


**Fig.12 Arrangement of Drift Pins (1) (Unit: mm)**

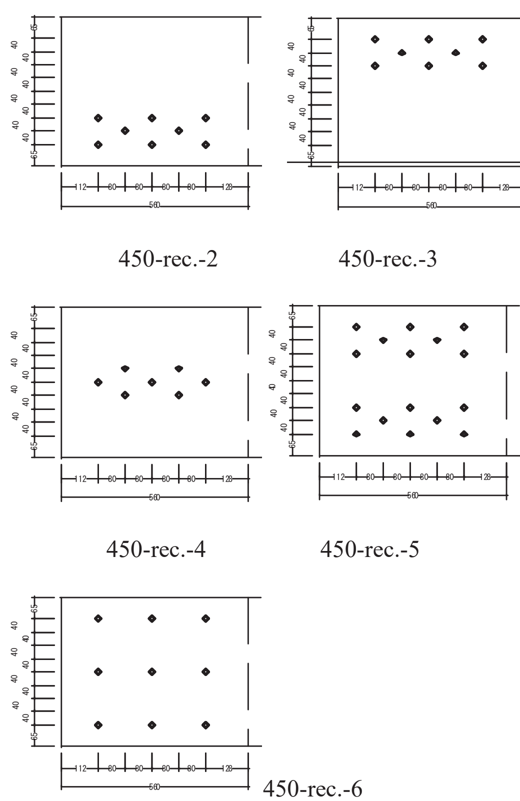


**Fig.13 Arrangement of Drift Pins (2) (Unit: mm)**



https://doi.org/10.52202/080513-0607

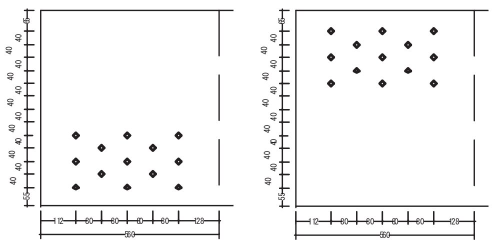

600-rec.-2 600-rec.-3

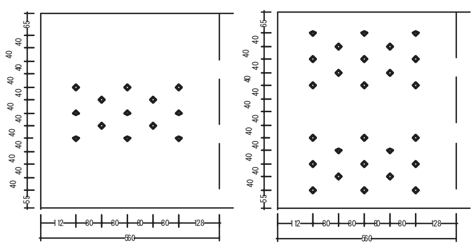

600-rec.-4 600-rec.-5

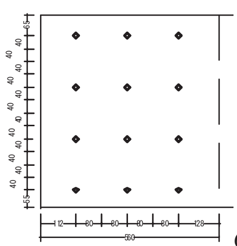

600-rec.-6

**Fig.14 Arrangement of Drift Pins (3) (Unit: mm)**

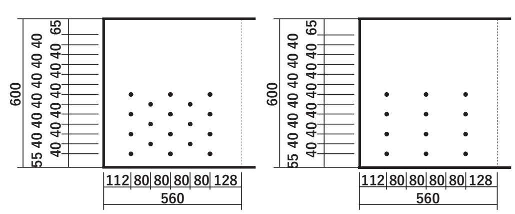


600-rec.7-1 600-rec.7-2

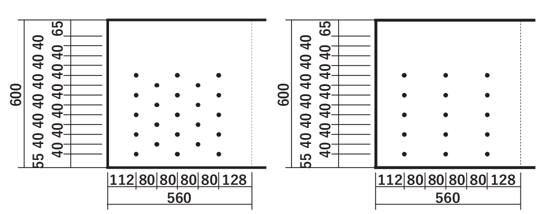


600-rec.8-1 600-rec.8-2

**Fig.15 Arrangement of Drift Pins (4) (Unit: mm)**

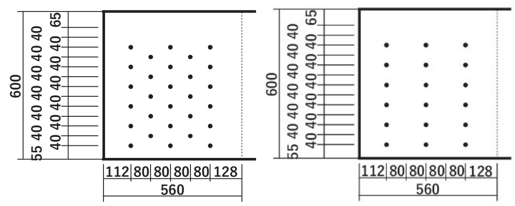


600-rec.9-1 600-rec.9-2

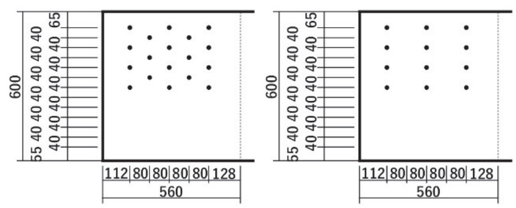


600-rec.10-1 600-rec.10-2

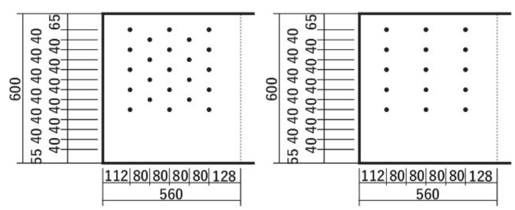


600-rec.11-1 600-rec.11-2

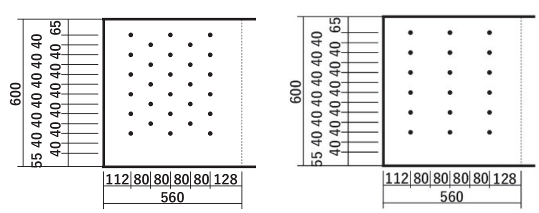


600-rec.12-1 600-rec.12-2

**Fig.16 Arrangement of Drift Pins (5) (Unit: mm)**

Examining Eq. (2) and (3), it is evident that both equations include the parameter $h_e$. This suggests that varying $h_e$ may influence the failure mode. Based on this concept, the drift pin arrangements for Phases 2 and 3 were designed accordingly, and tests were conducted.

## 4.2 Test results

This study examines splitting failure and shear failure in timber joints. The failure characteristics are illustrated in **Fig. 17**, while examples of the load-displacement relationships are presented in **Fig. 18 and 19**.

In this study, the failure characteristics were classified into two types. The first type is splitting failure, which originates from the drift pin farthest from the upper edge of the specimen. As shown in **Fig. 18**, this failure is accompanied by a sudden drop in load at a high load level. This load is defined as the splitting strength.

The second type is shear failure, which occurs at a different location than splitting failure. While shear failure is often accompanied by a loud sound, the load does not necessarily drop as significantly as in splitting failure. Instead, the load may increase again before either shear failure or splitting failure ultimately occurs. A characteristic feature of shear failure is the occurrence of displacement at the end grain of the specimen (This phenomenon is illustrated in the lower photograph of **Fig. 17**). In this study, the load at which shear failure first appears is defined as the shear strength.

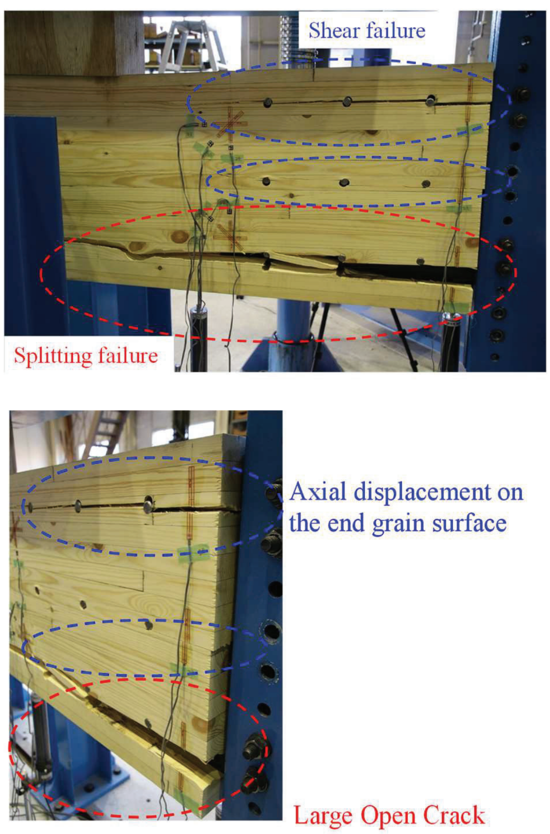


**Fig.17 Fracture conditions**

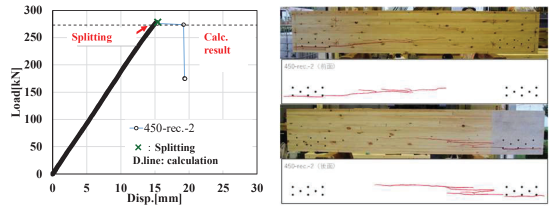


**Fig.18 Load-disp. Relationship and cracked area for splitting fracture**

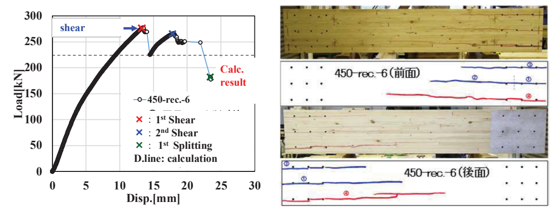


**Fig.19 Load-disp. Relationship and cracked area for shear fracture**

The classification of failure modes for all specimens is shown in **Fig. 20–23**. As illustrated in the figures, specimens with a larger $h_e$ tend to experience shear failure first, while those with a smaller $h_e$ are more likely to undergo splitting failure.

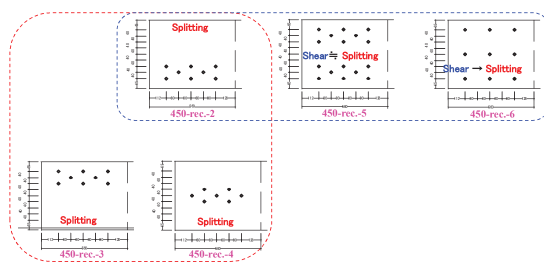


**Fig.20 Failure mode 1) (Depth:450mm)**

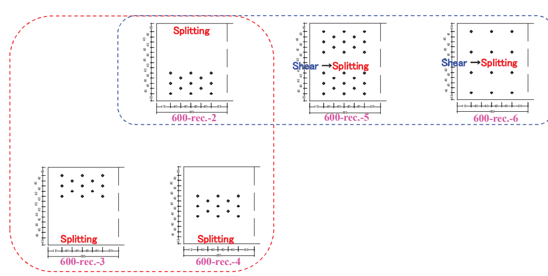


**Fig.21 Failure mode 2) (Depth:600mm)**


https://doi.org/10.52202/080513-0607

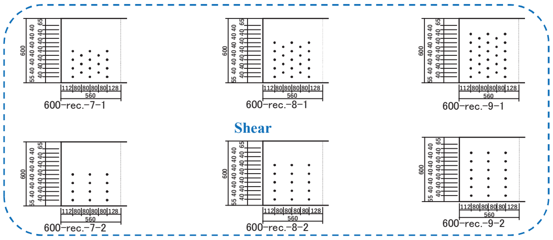


**Fig.22 Failure mode 3) (Depth:600mm)**

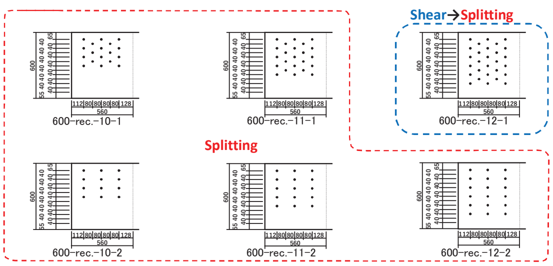


**Fig.23 Failure mode 4) (Depth:600mm)**

### 4.3 Discussion

Next, the values obtained from the material tests were input into Equations (2) and (3), and the calculated values were compared with the experimental results, as shown in **Fig. 24 (Splitting fracture) and Fig. 25 (Shear fracture)**. Here, the material values used for input were those specified in the Standard for Structural Design of Timber Structures(△), the 5% lower bound values from the material tests (○) and the average values from the material tests (×). The calculation results using the average material strength values showed instances where the evaluation was on the unsafe side.

For splitting failure, the values specified in the standard and the 5% lower bound values from material tests were nearly identical, resulting in similar estimation accuracy. Additionally, a positive correlation was observed between the experimental and calculated values.

For shear strength, the 5% lower bound value was approximately 1.4 times the value specified in the standard, resulting in a 1.4-fold difference in the calculated values as well.

As shown in these figures, a positive correlation was observed between the experimental and calculated values. Furthermore, calculations using the 5% lower bound value exhibited a higher estimation accuracy.

Finally, the smaller value from Equations (2) and (3) was taken as the design value, and the comparison between the design values and the experimental results is shown in **Fig. 26** (combined together with **Fig. 24 and 25**). As shown in the figure, when using the values specified in the current Standard for Structural Design of Timber Structures, a positive correlation is observed between the experimental and design values. However, when using the 5% lower bound values, the estimation accuracy is notably improved. Furthermore, by using the 5% lower bound values, the failure modes predicted by the equations largely corresponded with those observed in the experiments.

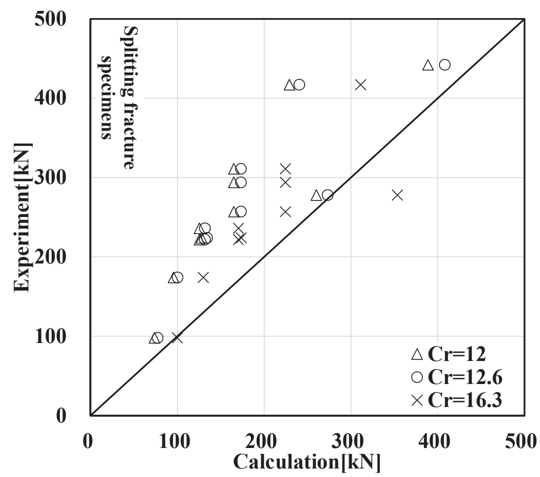


**Fig.24 Comparison with Exp. and Calc.**

**(Splitting failure)**

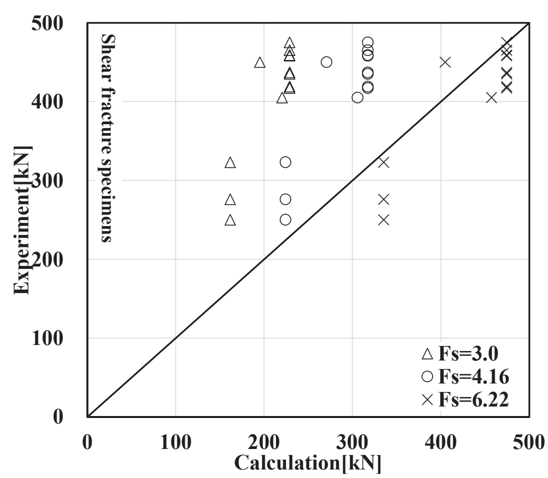


**Fig.25 Comparison with Exp. and Calc.**

**(Shear failure)**

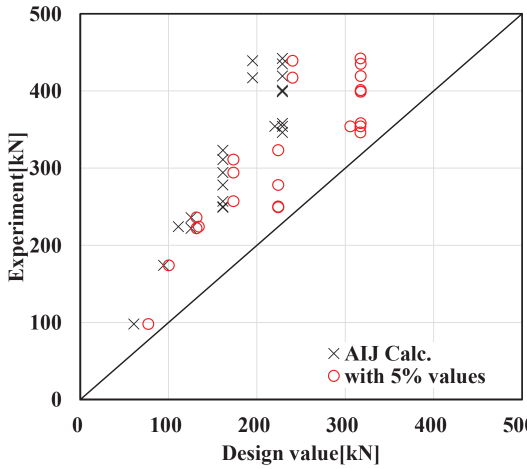


**Fig.26 Comparison with Exp. And Design values**

**(with All specimens)**

Among the test specimens, there were two cases where the failure mode predicted by the equations differed from the actual failure mode observed in the experiments. However, as shown in **Fig. 26**, this discrepancy does not pose any issues in the application of the design equations. This inconsistency is presumed to be due to the natural variability of wood, which can influence failure modes. Therefore, future studies will include statistical analysis to further investigate this phenomenon. Part of this study has been presented in our previous research [4].

## 5 – CONCLUSION

In this study, loading tests were conducted using steel-inserted connections with drift pins, focusing on splitting failure and shear failure. Through this investigation, the characteristics of splitting failure and shear failure were identified, and their respective strengths were determined.

To estimate these strengths, the appropriate material strength values were examined. The results indicated that, within the scope of this study, using the 5% lower bound values from material tests provided the highest estimation accuracy.

## 6 – ACKNOWLEDGMENTS

This work was supported by JSPS KAKENHI Grant Number JP 20H02303 and Taisei Foundation.

## 7 – REFERENCES

[1] Architectural Institute of Japan: Standard for Structural Design of Timber Structures, (2006) (Japanese)

[2] Japan Housing and Wood Technology Center: Manual for Strength Testing of Structural Timber, (2011) (Japanese).

[3] Japanese Agricultural Standard, 1152 (Japanese).

[4] W. KAMBE, K. SUZUKI, Y. OCHIAI, A. TAKINO, S. OKAMOTO, K. KOBAYASHI, K. SAWATA, S. NAKASHIMA, K. OGAWA and K. Tanaka “A Discussion of evaluation methods for splitting and shear failure by current standard equations for drift-pined joint with inserted plated plate at the end of gluelam-beam” In: J. Struct. Constr. Eng., AIJ, Vol. 90, No. 827, (2025), pp.94-103.(Japanese)


https://doi.org/10.52202/080513-0607